

QCD@Work 2014 will be set by the publisher

DOI: will be set by the publisher

© Owned by the authors, published by EDP Sciences, 2014

Bottomonium in the plasma

Lattice results

Gert Aarts¹, Chris Allton¹, Wynne Evans¹, Pietro Giudice², Tim Harris³, Aoife Kelly⁴, Seyong Kim⁵, Maria Paola Lombardo⁶, Sinead Ryan³, and Jon-Ivar Skullerud⁴

¹*Department of Physics, College of Science, Swansea University, Swansea SA2 8PP, U.K.*

²*Institut für Theoretische Physik, Universität Münster, D-48149 Münster, Germany*

³*School of Mathematics, Trinity College, Dublin 2, Ireland*

⁴*Department of Mathematical Physics, Maynooth University, Maynooth, Co.Kildare, Ireland*

⁵*Department of Physics, Sejong University, Seoul 143-747, Korea*

⁶*INFN, Laboratori Nazionali di Frascati, I-00044 Frascati, Italy*

Abstract. We present results on the heavy quarkonium spectrum and spectral functions obtained by performing large-scale simulations of QCD for temperatures ranging from about 100 to 500 MeV, in the same range as those explored by LHC experiments. We discuss our method and perspectives for further improvements towards the goal of full control over the many systematic uncertainties of these studies.

1 Introduction

Most ordinary hadrons can only exist up to temperatures of about 150–170 MeV. Beyond that, chiral symmetry is restored and confinement is lost. We know that this hot state of matter — the Quark-Gluon Plasma (QGP) — existed in the early universe: the transition from the QGP to the hadronic world is the latest cosmological transition. The QGP can be re-created in accelerators: the talk by Roberta Arnaldi [1] provides an excellent introduction into the status of this rich experimental program.

At low temperature the thermal medium consists of a gas of light pions, while towards infinite temperature quarks and gluons become free, with a corresponding increase of the pressure. After a debate lasting several years a consensus has been reached on how to interpolate between these two different, limiting regimes [2]. It turns out that there is a large intermediate temperature range which is not amenable to any analytic approaches, even when the most sophisticated high temperature expansions and model analyses are being used. This is the region explored by experiments, and this is where our lattice simulations are being performed.

Hadrons are of course dramatically affected in the QGP: the light quarks lose their dynamical masses and chiral partners approach degeneracy. Quark–antiquark states bound by long-distance, confining forces dissolve. It is very remarkable that heavy quarkonia behave very differently in this respect, as their fundamental states might well persist into the plasma: indeed heavy quarks and antiquarks are bound by short range Coulombic interactions which are not immediately affected by temperatures of the order of 200 MeV. Experimental evidence has been reviewed at this meeting [3] and our motivation is to provide a solid theoretical baseline for these studies.

A comprehensive review has recently appeared [4], and we concentrate here on our own recent work [5–8]. The next section is an introduction into spectral functions and related methodology. Then we give an overview of quarkonia in the Quark-Gluon Plasma. The following section is devoted to a more detailed presentation of the bottomonium results. We close with a brief discussion.

2 Relativistic and non-relativistic spectral functions

Spectral functions play an important role in understanding how elementary excitations are modified in a thermal medium. In a relativistic field theory approach the temperature T is realized through (anti)periodic boundary conditions in the Euclidean time direction and the spectral decomposition of a zero-momentum Euclidean propagator $G(\tau)$ at finite temperature is given by

$$G(\tau) = \int_0^\infty \frac{d\omega}{2\pi} K(\tau, \omega) \rho(\omega), \quad 0 \leq \tau < \frac{1}{T}, \quad (1)$$

where $\rho(\omega)$ is the spectral function and the kernel K is given by

$$K(\tau, \omega) = \frac{(e^{-\omega\tau} + e^{-\omega(1/T-\tau)})}{1 - e^{-\omega/T}}. \quad (2)$$

The τ dependence of the kernel reflects the periodicity of the relativistic propagator in imaginary time, as well as its T symmetry. The Bose–Einstein distribution, intuitively, describes the wrapping around the periodic box which becomes increasingly important at higher temperatures. When the significant ω range greatly exceeds the temperature, $K(\tau, \omega) \simeq (e^{-\omega\tau} + e^{-\omega(1/T-\tau)})$: backwards and forwards propagations are decoupled and the spectral relation reduces to

$$G(\tau) = \int_{\omega_0}^\infty \frac{d\omega'}{2\pi} \exp(-\omega'\tau) \rho(\omega'). \quad (3)$$

This approximation holds true in NRQCD: the interesting physics takes place around the two-quark threshold, $\omega \sim 2M \sim 8$ GeV for b quarks, which is still much larger than our temperatures $T < 0.5$ GeV. In our applications, following ref. [9], we will change variable $\omega = 2M + \omega'$.

Turning to the actual computational methodology, the calculation of the spectral functions using Euclidean propagators as an input is a difficult, ill-defined problem. We will tackle it using the Maximum Entropy Method (MEM) [10], which has proven successful in a variety of applications. We have studied the systematics carefully, including the dependence on the set of lattice data points in time, and on the default model $m(\omega)$ which enters in the parametrisation of the spectral function,

$$\rho(\omega) = m(\omega) \exp \sum_k c_k u_k(\omega), \quad (4)$$

where $u_k(\omega)$ are basis functions fixed by the kernel $K(\tau, \omega)$ and the number of time slices, while the coefficients c_k are to be determined by the MEM analysis [10]. We find that the results are insensitive to the choice of default model, provided that it is a smooth function of ω , and we will provide some examples in the next section.

Recently, an alternative Bayesian reconstruction of the spectral functions has been proposed in ref. [11, 12], and applied to the analysis of HotQCD configurations [13]. Some preliminary results for the bottomonium spectral functions obtained using this new reconstruction on our ensembles became available after the QCD@work meeting and have been presented at recent conferences [5, 6].

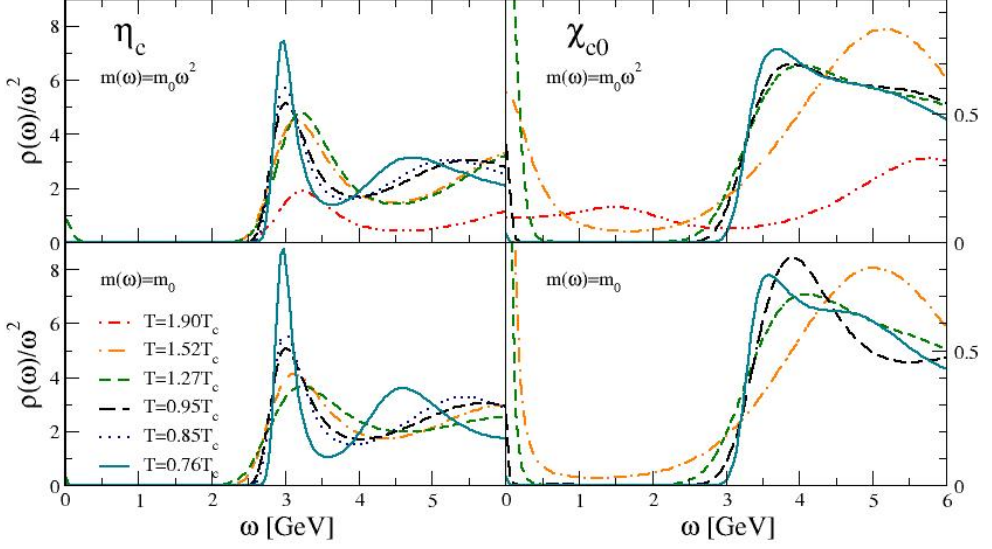


Figure 1. The spectral function for the charmonium states η_c (S-wave) and χ_{c0} (P-wave) for varying temperatures, using gauge field ensembles with dynamical u, d and s quarks. The results from two different default models are shown in the upper and lower diagrams respectively to demonstrate the stability of the analysis.

3 Overview of our quarkonium results

The results on bottomonium presented in this note should be framed in the broader context of studies of quarkonia as QCD thermometers, either from lattice first principles simulations, or from a lattice-informed potential model approach. Our most recent results for bottomonium [7] have been obtained by analysing gauge field configurations with two active light quarks and one heavier quark. The lighter quarks are still heavier than the physical up and down quarks as at $T = 0$, $m_\pi/m_\rho \simeq 0.4$, while the mass of the heavier quark is close to the strange mass. These results can be contrasted with earlier ones obtained with an infinite ‘strange’ mass (two active flavours) [14, 15]: in brief summary, we have found that the results from the different ensembles are broadly consistent, and we defer a more detailed comparison to future work.

The spectral functions of the charmonium states have been studied as a function of both temperature and momentum, using as input relativistic propagators with two light quarks [16, 17] and, more recently, including the strange quark. These most recent results are shown in fig. 1, for temperatures ranging between $0.76T_c$ and $1.9T_c$. The sequential dissolution of the peaks corresponding to the S- and P-wave states is clearly seen. Transport coefficients can be obtained from the low frequency domain, and this is an important aspect of our research [17, 18]. Furthermore, the inter-quark potential in charmonium was calculated using the HAL-QCD method, originally developed for the study of the nucleon–nucleon potential [19]. At low temperatures, we observe agreement with the Cornell potential, and the potential flattens (weakens), as expected, when the temperature increases. This is the first ab initio calculation of force between relativistic quarks as a function of temperature. The results are consistent with the expectation that charmonium melts at high temperature.

Bottomonium mesons have been studied using the NRQCD approximation for the bottom quark [20]. We defer the discussion of details to the next section, and here we focus on the main results

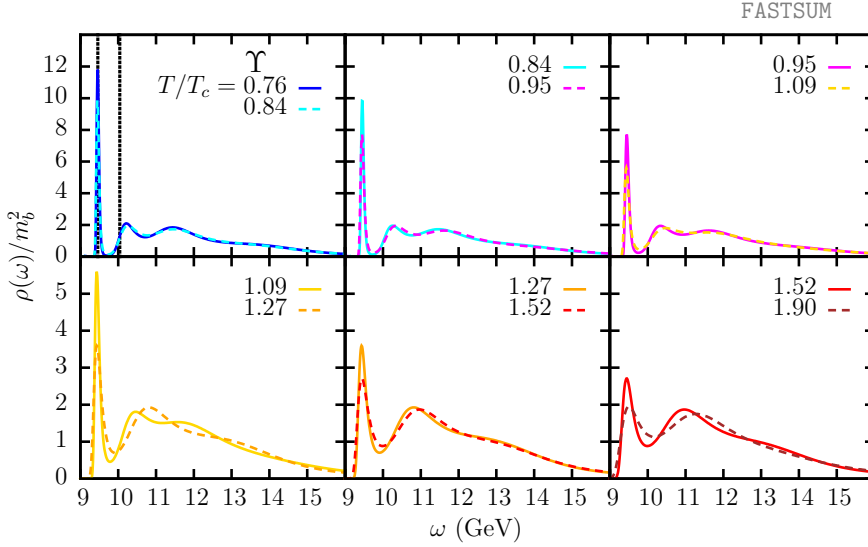


Figure 2. The spectral functions for the Υ at different temperatures, obtained using the maximum entropy method.

— the spectral functions. Note that in this case the low frequency limit is excluded: transport peaks are sensitive to long-distance, nearly constant modes and do not develop when winding along the Euclidean time direction is suppressed. The results [7] for the Upsilon shown in fig. 2 clearly demonstrate the persistence of the fundamental state above T_c as well as the suppression of the excited states. These patterns should be contrasted, for instance, with the one observed by the CMS experiment: for an estimated temperature of about 420 MeV the excited peaks of the invariant mass distribution are suppressed. Consider now the rate of production of muon pairs $\frac{dN_{\mu\bar{\mu}}}{d^4x d^4q} = F(q, T, \dots)\rho(\omega)$. The connection between the invariant mass distribution and the spectral function is clear, although the dynamical factor F is largely unknown. Understanding in detail this connection is an important aspect of ongoing research [21]. In the following we will limit ourselves to the presentation and discussion of our spectral functions. The comparison of important features of our results — masses, as seen in the central peak positions, and associated widths — with effective models is satisfactory, and gives us further confidence in our analysis.

Our results for the P -wave χ_{b1} [7] are shown in fig. 3. Here checks of the systematic errors are still in progress, and in particular we would like to assess the fate of the fundamental state at T_c , possibly before experimental results — which are still lacking in this sector — appear!

4 Bottomonium in the plasma — some details on our analysis

We discuss here in more detail our results for the Upsilon and the χ_b . The analysis starts with the computation of the correlators in Euclidean time within the NRQCD formalism, which in turn are input to the spectral functions presented above.

NRQCD is an effective field theory with power counting in the heavy quark velocity in the bottomonium rest frame. The heavy quark and anti-quark fields decouple and their numbers are separately conserved. Their propagators, $S(x)$, solve an initial-value problem whose discretization leads

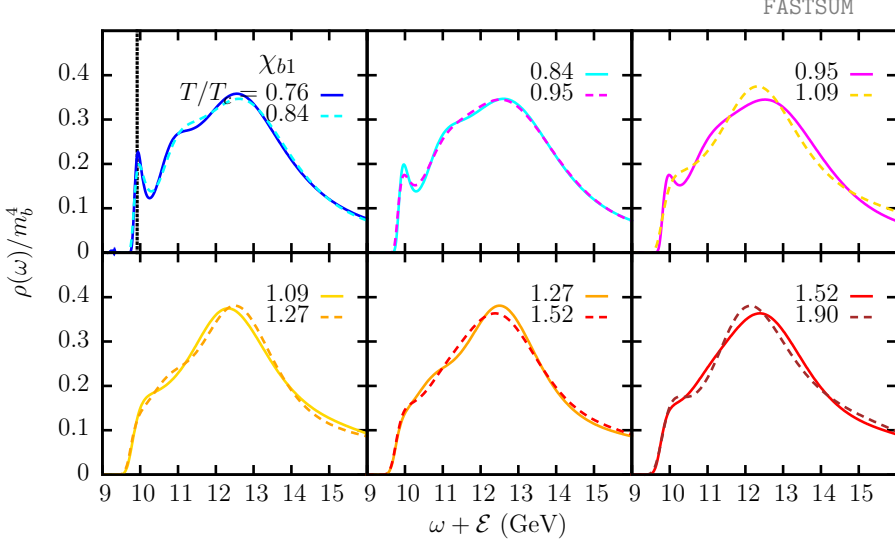


Figure 3. The spectral functions for the χ_b at different temperatures, obtained using the maximum entropy method.

to the following choice for the evolution equation

$$S(x + a_\tau e_\tau) = \left(1 - \frac{a_\tau H_0|_{\tau+a_\tau}}{2k}\right)^k U_\tau^\dagger(x) \left(1 - \frac{a_\tau H_0|_\tau}{2k}\right)^k (1 - a_\tau \delta H) S(x), \quad (5)$$

where $U_\tau(x)$ is the temporal gauge link at site x and e_τ the temporal unit vector. The leading order Hamiltonian is defined by $H_0 = -\frac{\Delta^{(2)}}{2m_b}$, with $\Delta^{(2n)} = \sum_{i=1}^3 (\nabla_i^\dagger \nabla_i)^n$. The higher order covariant finite differences are written in terms of the components of the usual forward and backward first order ones. Further details can be found e.g. in ref. [7]. Only energy differences are physically significant in NRQCD because the rest-mass energy can be removed from the heavy quark dispersion relation by performing a field transformation. Since there is no rest mass term in the NRQCD action one can dispense with the demanding constraint $a \ll 1/m_b$.

In our most recent work [7] we have tuned the heavy quark mass by requiring the spin-averaged 1S kinetic mass, $M_2(\overline{1S}) = (M_2(\eta_b) + 3M_2(\Upsilon))/4$, to be equal to its experimental value. The tuned value of the heavy quark mass corresponds to $M_2(\overline{1S}) = 9560(110)$ MeV which is consistent with the experimental value, $M_{\text{expt}}(\overline{1S}) = 9444.7(8)$ MeV.

We now turn to the analysis of correlators. Consider first the infinite temperature limit, i.e. the limiting case of free heavy quarks: in continuum NRQCD the spectral functions are known [9], and are given by¹

$$\rho_{\text{free}}(\omega) \propto (\omega - \omega_0)^\alpha \Theta(\omega - \omega_0), \quad \text{where} \quad \alpha = \begin{cases} 1/2, & \text{S wave;} \\ 3/2, & \text{P wave.} \end{cases} \quad (6)$$

¹We have included a threshold, ω_0 , to account for the additive shift in the quarkonium energies. For free quarks the threshold occurs at $2m_b$, which within NRQCD corresponds to $\omega_0 = 0$.

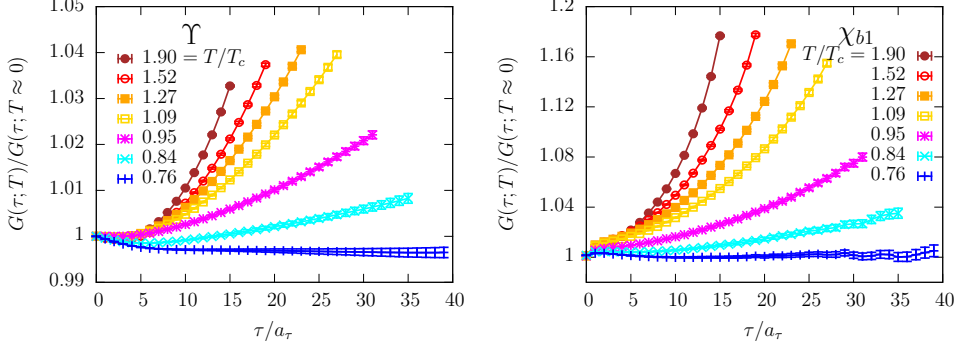


Figure 4. Thermal modification, $G(\tau; T)/G(\tau; T \approx 0)$, of the correlation functions in the Υ (left) and χ_{b1} (right) channels.

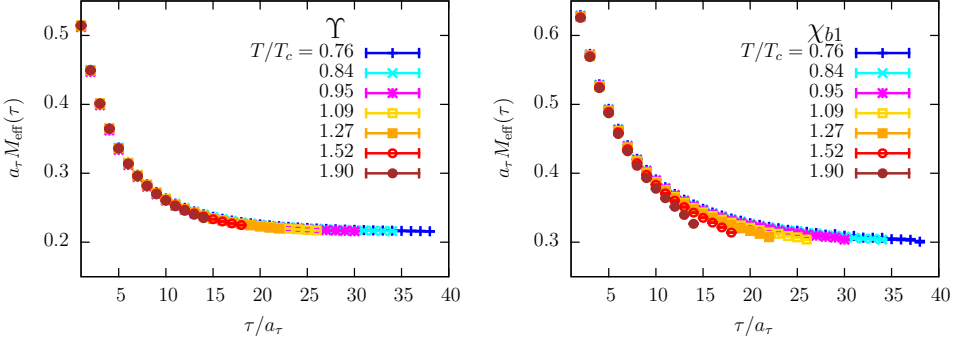


Figure 5. Temperature dependence of the effective mass in the Υ (left) and the χ_{b1} (right) channels.

The correlation functions then have the following behaviour

$$G_{\text{free}}(\tau) \propto \frac{e^{-\omega_0 \tau}}{\tau^{\alpha+1}}. \quad (7)$$

To show their temperature dependence we consider the ratios of the correlation functions at finite temperature to those at zero temperature. They are shown in fig. 4. We see that the thermal modifications are much larger in the P-wave than in the S-wave channel. A useful numerical tool is the so-called effective mass $M_{\text{eff}}(\tau)$:

$$M_{\text{eff}}(\tau) \equiv -\frac{1}{G(\tau)} \frac{dG(\tau)}{d\tau} \xrightarrow{G=G_{\text{free}}} \omega_0 + \frac{\alpha+1}{\tau}. \quad (8)$$

The results are shown in fig. 5. The S-wave effective mass displays little temperature dependence (left) but a clear effect is seen in the P-wave channel effective mass (right). In ref. [20] it was also observed that the S-wave effective mass showed little variation with temperature while the temperature dependence in the P-wave channel effective mass was even more pronounced than visible here.

These results clearly show a temperature dependence, but it is not easy to assess with confidence the fate of bound states. While in real time the information on the long term dynamics is fully accessible, in imaginary time all the information is squeezed within the periodicity $\tau_P = 1/T$. One would

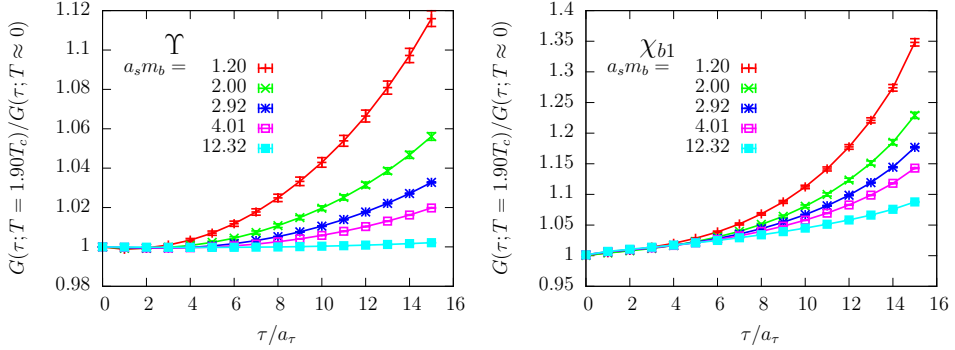


Figure 6. Dependence on the heavy quark mass of the modification in the correlators at the highest accessible temperature, $T/T_c = 1.90$, in the Υ (left) and χ_{b1} (right) channels.

need an extremely high accuracy on extremely fine lattices to make quantitative statements from the correlators alone. This further motivates an analysis in terms of spectral functions.

5 Discussion

In summary, we have a coherent scenario for the Υ : the fundamental state survives up to at least twice the critical temperature, while the excited states dissolve. With the caveats mentioned above, this is consistent with the observations of CMS, ALICE and PHENIX. The fundamental state has some modifications whose basic features can be captured by effective field theories. However, at a temperature of about 420 MeV ALICE results [3] indicate that the suppression of Υ and J/ψ as a function of the number of participants is comparable, within the present uncertainties. This can be explained by the J/ψ being more suppressed, but also more sensitive to regeneration, the two effects competing in such a way that the resulting R_{AA} is similar to that of the Υ . When comparing RHIC and LHC results, it is found that the nuclear modification factor at RHIC is smaller than at the LHC — the so called quarkonium suppression puzzle. New theoretical ideas have been put forward to interpret this behaviour [22]. All this confirms the interest in ab initio lattice studies of charmonia and bottomonia in hot matter with full control of systematical errors. On the lattice we might also take advantage of the freedom to simulate arbitrary masses: some preliminary results were presented in ref. [23] and the most recent ones [7] are shown in fig. 6. Guided by these analysis we might be able to locate a melting line in the temperature–mass plane which passes through the individual melting temperatures observed in different channels. These studies might help unravel general features of the dissolutions of heavy states and their interrelation with gauge dynamics.

One important next step is a full control over matter content in our lattice simulations. The simulations reported here have been performed with $\frac{m_\pi}{m_\rho} \simeq 0.4$, and with m_s either set to infinity or to its physical value. We aim at physical $m_{u,d,s}$ masses which should correspond to the correct matter content in the range $T \leq 400$ MeV. Above 400 MeV a dynamical charm quark might become relevant as well.

We have already mentioned the subtleties related with the reconstruction of the spectral functions. To gain confidence in our analysis we will continue cross checking MEM results with those based on the novel Bayesian approach [5, 6, 12]; applications of a generalised integral transform might ease the inversion task [24]; and model calculations will provide very useful testbeds for these new techniques [25, 26].

Acknowledgements It is a pleasure to thank Yannis Burnier and Alexander Rothkopf for many useful discussions. MpL wishes to thank the organisers of QCD@Work 2014 for their very nice hospitality and a most interesting meeting. AK acknowledges financial support through the Irish Research Council.

References

- [1] R. Arnaldi, this Volume
- [2] H. T. Ding, arXiv:1408.5236 [hep-lat].
- [3] I. Das, this Volume
- [4] A. Andronic, arXiv:1409.5778 [nucl-ex] and references therein
- [5] FASTSUM+, T. Harris *et al.*, talk presented by T. Harris at *Lattice 2014*, to appear in the Proceedings
- [6] FASTSUM+, J.-I. Skullerud *et al.*, talk presented by J.-I. Skullerud at *Confinement 2014*, to appear in the Proceedings
- [7] G. Aarts, C. Allton, T. Harris, S. Kim, M. P. Lombardo, S. M. Ryan and J. I. Skullerud, JHEP **1407** (2014) 097
- [8] G. Aarts, C. Allton, S. Kim, M. P. Lombardo, S. M. Ryan and J.-I. Skullerud, JHEP **1312** (2013) 064
- [9] Y. Burnier, M. Laine and M. Vepsalainen, JHEP **0801** (2008) 043
- [10] M. Asakawa, T. Hatsuda and Y. Nakahara, Prog. Part. Nucl. Phys. **46** (2001) 459
- [11] A. Rothkopf, J. Comput. Phys. **238** (2013) 106
- [12] Y. Burnier and A. Rothkopf, Phys. Rev. Lett. **111**, no. 18, 182003 (2013)
- [13] S. Kim, P. Petreczky and A. Rothkopf, arXiv:1409.3630 [hep-lat]
- [14] G. Aarts, C. Allton, S. Kim, M.P. Lombardo, M.B. Oktay, S.M. Ryan, D.K. Sinclair and J.-I. Skullerud, JHEP **1111** 103
- [15] G. Aarts, C. Allton, S. Kim, M. P. Lombardo, M. B. Oktay, S. M. Ryan, D. K. Sinclair and J.-I. Skullerud, JHEP **1303** 084
- [16] G. Aarts, C. Allton, M. B. Oktay, M. Peardon and J. I. Skullerud, Phys. Rev. D **76** (2007) 094513
- [17] A. Kelly, J. I. Skullerud, C. Allton, D. Mehta and M. B. Oktay, PoS LATTICE **2013** (2013) 170
- [18] A. Amato, G. Aarts, C. Allton, P. Giudice, S. Hands and J. I. Skullerud, Phys. Rev. Lett. **111** (2013) 172001
- [19] P. W. M. Evans, C. R. Allton and J.-I. Skullerud, Phys. Rev. D **89** (2014) 071502
- [20] G. Aarts, S. Kim, M. P. Lombardo, M. B. Oktay, S. M. Ryan, D. K. Sinclair and J.-I. Skullerud, Phys. Rev. Lett. **106** (2011) 061602
- [21] F. Antinori, N. Armesto, P. Bartalini, R. Bellwied, P. Braun-Munzinger, B. Cole, A. Dainese and M. Gazdzicki *et al.*, arXiv:1409.2981 [hep-ph]
- [22] D. E. Kharzeev, arXiv:1409.2496 [hep-ph]
- [23] S. Kim, G. Aarts, C. Allton, M. P. Lombardo, M. B. Oktay, S. M. Ryan, D. K. Sinclair and J. I. Skullerud, PoS LATTICE **2012** (2012) 086
- [24] F. Pederiva, A. Roggero and G. Orlandini, Phys. Rev. **B88** (2013) 094302; J. Phys. Conf. Ser. **527** (2014) 012011
- [25] P. Colangelo, F. Giannuzzi and S. Nicotri, JHEP **1205** (2012) 076
- [26] F. Giannuzzi, arXiv:1409.2528 [hep-ph]